

See discussions, stats, and author profiles for this publication at: <https://www.researchgate.net/publication/215477037>

Light Scattering and NMR Studies on the Self-Aggregation of Sodium n -Hexyl Sulfate in Aqueous Electrolyte Solution

ARTICLE *in* LANGMUIR · FEBRUARY 2000

Impact Factor: 4.46 · DOI: 10.1021/la990721f

CITATIONS

19

READS

36

5 AUTHORS, INCLUDING:



Juan M. Ruso

University of Santiago de Compostela

163 PUBLICATIONS 2,042 CITATIONS

SEE PROFILE



Pablo Taboada

University of Santiago de Compostela

149 PUBLICATIONS 2,317 CITATIONS

SEE PROFILE



Víctor Mosquera

University of Santiago de Compostela

170 PUBLICATIONS 3,114 CITATIONS

SEE PROFILE



Félix Sarmiento

University of Santiago de Compostela

158 PUBLICATIONS 2,485 CITATIONS

SEE PROFILE

Light Scattering and NMR Studies on the Self-Aggregation of Sodium *n*-Hexyl Sulfate in Aqueous Electrolyte Solution

Juan M. Ruso, David Attwood,[†] Pablo Taboada, Víctor Mosquera, and Félix Sarmiento*

Grupo de Física de Coloides y Polímeros, Departamento de Física Aplicada y Departamento de Física de la Materia Condensada, Facultad de Física, Universidad de Santiago de Compostela, E-15706 Santiago de Compostela, Spain, and School of Pharmacy and Pharmaceutical Sciences, University of Manchester, Manchester M13 9PL, U.K.

Received June 8, 1999. In Final Form: October 19, 1999

The self-aggregation of sodium *n*-hexyl sulfate (SHS) in aqueous solution has been studied from static and dynamic light scattering and ¹H nuclear magnetic resonance (NMR) at 25 °C in the presence of added electrolyte concentration (0.0–0.5 mol kg⁻¹ NaCl). Critical concentrations, aggregation numbers, effective aggregate charges, and degrees of aggregate ionization have been calculated, with similar results from each of the different techniques. The interaction between aggregates was interpreted from diffusion data from dynamic light scattering using DLVO theory. Aggregation properties have been determined by application of mass action theory to the concentration dependence of ¹H NMR chemical shifts, confirming the results obtained by the light scattering techniques.

Introduction

Although early researchers seemed to indicate that aqueous solutions of surfactants with short hydrocarbon chains contain nonaggregated molecules¹ in recent works we have reported in studies of the association characteristics and thermodynamic properties of aqueous solutions of *n*-hexyltrimethylammonium bromide (C₆TAB)² and sodium *n*-hexyl sulfate (SHS),³ that both of these solutions form small aggregates at a critical concentration.

In our study of SHS we demonstrated the aggregation properties in water by measurement of conductivities, enthalpy changes on aggregation, densities, ultrasound velocities, and surface tension.³ From these data critical concentrations (*c*_c), degree of counterion binding, Gibbs energy and entropy change on aggregation, apparent and partial molal volumes, apparent adiabatic compressibilities, and surface properties were calculated. These properties were compared with those of other members of the alkyl sulfate series and a linear variation with the number of carbon atoms (*n*_C) in the alkyl chain was found. For example, standard enthalpies of micellization decrease in 0.7 kJ mol⁻¹ per methylene group, apparent molal volume at infinite dilution increases in approximately 16 cm³ mol⁻¹ and the critical micelle concentration (cmc) decreases by a factor close to 2. To obtain a more complete characterization of this system, we now extend this work using different techniques and examining the influence of electrolyte on the aggregation behavior of the SHS. The concentration of added electrolyte was restricted to less than 0.5 mol kg⁻¹ NaCl. We have used dynamic light scattering to determine diffusion coefficients and have

interpreted the data using the Corti and Degiorgio⁴ treatment based on the Derjaguin–Landau–Verwey–Overbeek (DLVO) theory of colloid stability.⁵ This theory permits us to quantify the interactions between aggregates by means of the interaction potential, which consists of a hard-sphere repulsive part, an electrostatic long-range repulsion, and a London–van der Waals attraction. It contains only two unknown parameters, the electric potential at the shear surface of the aggregate and the Hamaker constant. These parameters have been calculated with a computational procedure. The importance of including the contribution of counterions from the surfactant in these calculations has been examined.

To obtain further information on the structure and dynamics of the aggregates we have used ¹H NMR spectroscopy, which has been recognized to be an important tool in the study of association of surfactants.^{6–8} Critical concentrations and aggregation numbers were determined from chemical shift data for each of four positions of protons along the alkyl chain of SHS.

Experimental Section

Materials. Sodium *n*-hexyl sulfate was obtained from Lancaster Synthesis Ltd. (no. 6245). Purity of the compound was better than 99% and was used as received without further purification. Water was double-distilled, deionized, and degassed before use. Sodium chloride obtained from Fluka was of analytical grade.

Light Scattering Measurements. Static light scattering measurements were made at 298 ± 0.1 K using a Malvern 7027 laser light scattering instrument equipped with a 2-W argon ion laser (Coherent Innova 90) operating at 488 nm with vertically polarized light. Solutions were clarified by ultrafiltration through 0.1 μm filters with the ratio of light scattering at angles of 45° and 135° not exceeding 1.10.

The refractive index increments of the sodium *n*-hexyl sulfate aggregates were measured at 298 ± 0.1 K using an Abbé 60/DE

* To whom correspondence should be addressed. Tel.: +34 981 563 100. Fax: +34 981 520 676. E-mail: fsarmio@usc.es.

[†] University of Manchester.

(1) Williams, E.; Sears, B.; Allerhand, A.; Cordes, E. H. *J. Am. Chem. Soc.* **1973**, *95*, 4871.

(2) Mosquera, V.; del Río, J. M.; Attwood, D.; García, M.; Jones, M. N.; Prieto, G.; Suárez, M. J.; Sarmiento, F. *J. Colloid Interface Sci.* **1998**, *206*, 66.

(3) Suárez, M. J.; López-Fontán, J. L.; Sarmiento, F.; Mosquera, V. *Langmuir* **1999**, *15*, 5265.

(4) Corti, M.; Degiorgio, V. *J. Phys. Chem.* **1981**, *85*, 711.

(5) Verwey, E. J. W.; Overbeek, J. T. G. In *Theory of the Stability of Lyophobic Colloids*; Matijevic, E., Ed.; Wiley: New York, 1948.

(6) Nakagawa, T.; Tokiwa, F. In *Surface and Colloid Science*; Matijevic, E., Ed.; Wiley: New York, 1976.

(7) Wennerston, H.; Lindman, B. *Phys. Rep.* **1979**, *52*, 1.

(8) Lindman, B.; Wennerston, H. *Top. Curr. Chem.* **1980**, *87*, 1.

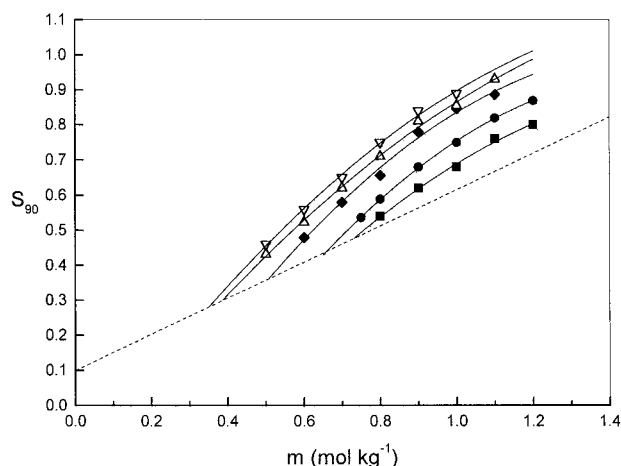


Figure 1. Variation of the scattering ratio, S_{90} , with concentration, m , for sodium *n*-hexyl sulfate in (■) water and in aqueous NaCl solutions of concentrations (●) 0.2; (◆) 0.3; (△) 0.4; and (▽) 0.5 mol kg⁻¹ at 298 K. (---) Monomer line.

Table 1. Critical Concentrations, (cc), Aggregation Numbers, (N) and Effective Aggregate Charges (z) of Sodium *n*-Hexyl Sulfate in Aqueous Electrolyte Solution at 298 K from Static Light Scattering

[NaCl] (mol kg ⁻¹)	cc (mol kg ⁻¹)	N	z
0.0	0.72	2	1.68
0.2	0.66	3	2.07
0.3	0.51	4	2.61
0.4	0.38	6	3.84
0.5	0.35	8	4.84

precision refractometer (Bellingham and Stanley Ltd.), giving a variation with concentration of 0.0251 ± 0.0004 kg mol⁻¹. Measurements in the most concentrated electrolyte solutions showed no effect of electrolyte on the value of the refractive increment within the limits of error of measurement. A value of 0.0104 kg mol⁻¹ was taken from the literature⁹ for the refractive index increment of NaCl.

Dynamic Light Scattering. Measurements were made at 298 ± 0.1 K and at a scattering angle of 90° with the Malvern instrument described above combined with a Brookhaven BI 9000AT digital correlator with a sampling time range of 25 ns to 40 ms. Solutions were clarified as described above. Diffusion coefficients were determined from a single-exponential fit to the correlation curve. Hydrodynamic radii were calculated from measured diffusion coefficients by means of the Stokes–Einstein equation.

Nuclear Magnetic Resonance. ¹H NMR was recorded on a JEOL EX270 270 MHz spectrometer at 293 ± 0.1 K. D₂O was used as solvent for all the experiments (Goss Scientific Instrument, Ltd.). The chemical shifts of peaks of interest were determined using a peak pick utility. The chemical shifts of peaks with heights exceeding the peak threshold were recorded by the computer. The peak threshold was set just below the top of the smallest peak of interest. All spectra were compared with sodium 3-(trimethylsilyl)propionate (TSP) which acted as an internal standard.

Results and Discussion

In Figure 1 the variation of the intensity of scattered light, S_{90} , (where S is the intensity of light scattered from a solution at 90° relative to the scattering from benzene) as a function of the sodium *n*-hexyl sulfate concentration, m , at electrolyte concentrations between 0.0 and 0.5 mol kg⁻¹ NaCl are shown.

The critical concentrations, corresponding to the intersection of the scattering curve and the theoretical line

(shown by a dashed line in Figure 1) representing ideal scattering from monomers are given in Table 1. The aggregation numbers, N , and effective aggregate charges, z , were calculated according to the Anacker and Westwell¹⁰ treatment, in which the light scattering from solutions of ionic aggregates is represented by

$$\frac{K' m_2}{\Delta R_{90}} = \frac{2m_3 + N^{-1}(z_1 + z_1')m_2}{[2N + (2N)^{-1}(z_1 + z_1')f^2 - 2fz]m_3 + z_1 m_2} \quad (1)$$

where ΔR_{90} is the Rayleigh ratio of the solution in excess of the critical concentration to a solution at the cc , m_2 is the molality of the aggregate species in terms of monomer, m_3 is the molality of the supporting electrolyte, and $f = (dn/dm_3)_{m_2}/(dn/dm_2)_{m_3}$. K' for vertically polarized incident light is defined by

$$K' = 4\pi^2 n_0^2 (dn/dm_2)_{m_3}^2 V^0 / N_A \lambda^4 \quad (2)$$

with n_0 being the refractive index of the solvent, V^0 the volume of solution containing 1 kg of water, N_A Avogadro's number, and λ the wavelength of the incident light (488 nm). Expansion of eq 1 in powers of m_2 leads to

$$\frac{K' m_2}{\Delta R_{90}} = A + B m_2 + \dots \quad (3)$$

where

$$A = 4N[(2N - fz_1)^2 + z_1 f^2]^{-1} \quad (4)$$

and

$$B = z_1 A (2m_3)^{-1} [(1 + z_1)N^{-1} - A] \quad (5)$$

Table 1 shows the obtained results.

Values (per mole of monomer) of the standard Gibbs energy change, ΔG_m^0 , on aggregation were calculated from the following expression, as predicted from the mass action model¹¹

$$\Delta G_m^0 = (2 - \alpha)RT \ln X_{cc} \quad (6)$$

where X_{cc} is the cc expressed in units of mol fraction and α is the degree of aggregate ionization ($\alpha = z/N$). In Figure 2 we show the plot of standard Gibbs energy change against the electrolyte concentration. Experimental points were fitted to a first degree polynomial with a correlation coefficient greater than 0.998.

Standard free energies of aggregation were also derived by the application of the mass action model using the equation¹²

$$\log cc = -(1 - \alpha) \log [X^-] + (\Delta G_m^0 / 2.303) + (1/N) \log F(m^{+p}) \quad (7)$$

where m^{+p} is the mol fraction of micelles and F is a term involving the activity coefficients of all species in solution. Plots of $\log cc$ against \log (counterion concentration), $\log [X^-]$, were linear (Figure 3) giving ΔG_m^0 and α values of -12.73 kJ mol⁻¹ and 0.70, respectively. These values are in reasonable agreement with those obtained by conductivity measurements,³ -14.80 kJ mol⁻¹ and 0.7 respec-

(10) Anacker, E. W.; Westwell, A. E. *J. Phys. Chem.* **1964**, *68*, 3490.

(11) Mitchell, D. J.; Ninham, B. W. *J. Chem. Soc., Faraday Trans.* **1981**, *77*, 601.

(12) Moroi, Y. *J. Colloid Interface Sci.* **1988**, *122*, 308.

(9) Kruis, A. Z. *Phys. Chem. B* **1936**, *34*, 13.

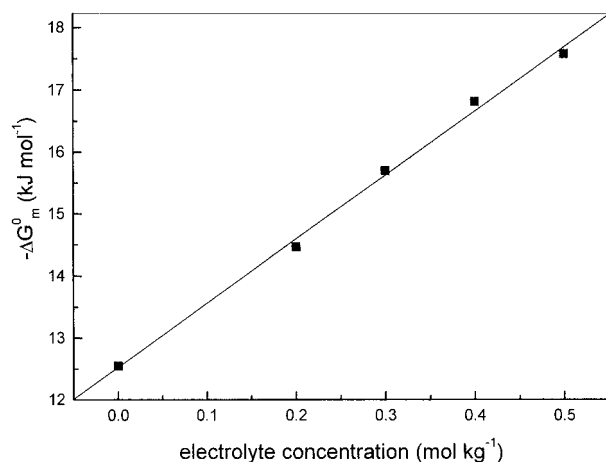


Figure 2. Change in standard Gibbs energy of aggregation, ΔG_m^0 , of sodium *n*-hexyl sulfate as a function of electrolyte concentration.

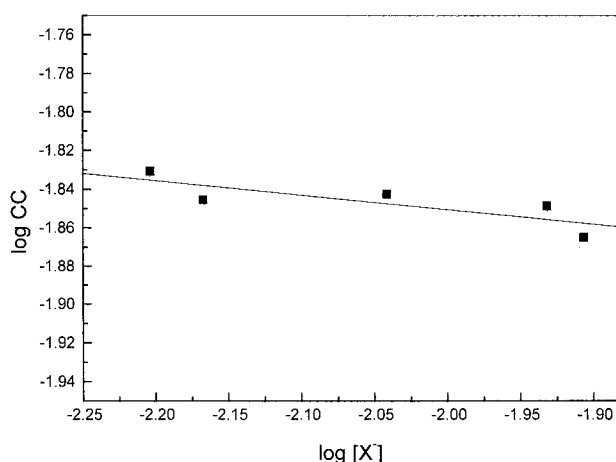


Figure 3. Logarithm of critical concentration from static light scattering as a function of logarithm of counterion concentration, $[X^-]$.

tively), the differences arising from the dependence of the critical concentration values on the method of determination. As expected, the value of the free energy of aggregation for SHS is lower than those of the other members of the sodium alkyl sulfate series,^{13–17} values of which decrease with the alkyl chain length, as can be seen in Figure 4, where our ΔG_m^0 values have been plotted with those of the literature. It is interesting to note the great similarity between the free energy for SHS and that obtained for the *n*-hexyltrimethylammonium bromide,² ($\Delta G_m^0 = -12.40 \text{ kJ mol}^{-1}$), which suggests that the major contribution to this energy is from the alkyl chain.

Apparent diffusion coefficients, D , of sodium *n*-hexyl sulfate in water and aqueous electrolyte solutions are presented in Figure 5 as a function of critical concentration ($m - cc$, where m is the total surfactant concentration).

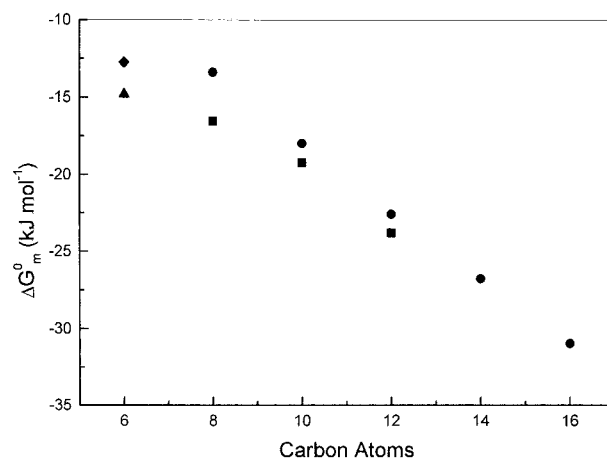


Figure 4. Gibbs energies of micellization as a function of carbon atoms in the alkyl chain length for *n*-alkyl sulfate series, (■) ref 14; (●) ref 15; (▲) ref 4; (◆) this work.

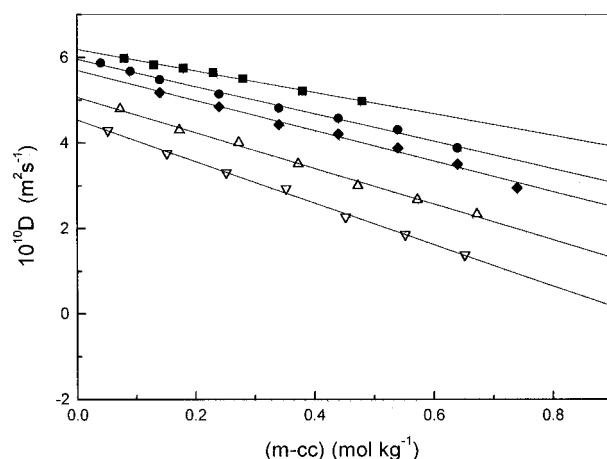


Figure 5. Diffusion coefficient, D , as a function of the aggregate concentration for sodium *n*-hexyl sulfate in (■) water and in aqueous NaCl solutions of concentrations (●) 0.2, (◆) 0.3, (△) 0.4 and (▽) 0.5 mol kg⁻¹ at 298 K.

Experimental data have been fitted with the linear function

$$D = D_0[1 + k_D(m - cc)] \quad (8)$$

where D_0 is the limiting diffusion coefficient at the critical concentration. To avoid the potential source of error caused by the contribution of monomers to the effective value of D , measurements were restricted to a concentration in which D was a linear function of molality.¹⁸ The concentration dependence of D is due to aggregate interactions. The limiting diffusion coefficients and the hydrodynamic radii, r_h , were derived from the Stokes–Einstein relationship

$$r_h = \frac{k_B T}{6\pi\eta D_0} \quad (9)$$

where k_B is the Boltzmann constant, T the temperature, and η the solvent viscosity. Table 2 shows an increase of hydrodynamic radius as a function of added salt concentration. The length of the SHS molecules, obtained by the empirical equation¹⁹ $l = 1.5 + 1.265n_c$, where l (in Å) is the chain length and n_c the number of carbon atoms, was 0.91 nm, which correspond to approximately two times the hydrodynamic radius and suggest a shape near to spherical for the aggregate surrounded by water molecules.

(13) Kresheck, G. C.; Hargraves, W. A. *J. Colloid Interface Sci.* **1974**, *48*, 481.

(14) Aniansson, E. A. G.; Wall, S. N.; Almgren, M.; Hoffman, H.; Kielmann, I.; Ulbricht, W.; Zana, R.; Lang, J.; Tondre, C. *J. Phys. Chem.* **1976**, *80*, 905.

(15) Paredes, S.; Tribout, M.; Ferreira, J.; Leonis, J. *Colloid Polymer Sci.* **1976**, *254*, 637.

(16) Eatough, D. J.; Rehfeld, S. J. *Thermochim. Acta* **1971**, *2*, 443.

(17) Sharma, V. K.; Bhat, R.; Ahluwalia, J. C. *J. Colloid Interface Sci.* **1978**, *115*, 396.

(18) Attwood, D.; Fletcher, P. J. *Colloid Interface Sci.* **1987**, *115*, 104.

(19) Tanford, C. *J. Phys. Chem.* **1972**, *76*, 3020.

Table 2. Limiting Diffusion Coefficient, D_0 , and Hydrodynamic Radius, r_h , of Sodium *n*-Hexyl Sulfate in Aqueous Electrolyte Solution at 298 K

[NaCl] (mol kg ⁻¹)	$10^{10} D_0$ (m ² s ⁻¹)	r_h (nm)	r_h (SDS) ^a (nm)
0.0	6.19	0.39	—
0.2	5.95	0.41	2.55
0.3	5.72	0.43	2.60
0.4	5.07	0.48	2.69
0.5	4.53	0.54	2.79

^a Values from ref 5.

To correlate experimental results of diffusion with the interactive forces between aggregates the data were analyzed according to the treatment proposed by Corti and Degiorgio.⁴ For interacting particles, the concentration dependence of D can be expressed in term of the volume fraction ϕ of the particles

$$D = D_0(1 + k_D\phi) \quad (10)$$

where $k_D = k_D/\bar{v}$ and is the specific volume of the solute particles as determined from density measurements at $m > cc$. k_D may be related to the pair interaction potential, $V(x)$, between spherical particles of radius a (equal to r_h) using the expression proposed by Felderhof²⁰

$$k_D = 1.56 +$$

$$\int_0^\infty [24(1+x)^2 - F(x)][1 - \exp(-V(x)/k_B T)] dx \quad (11)$$

where $x = (R - 2a)/2a$, R is the distance between the centers of two particles, and $F(x)$ is given as

$$F(x) = 12(1+x) - \frac{15}{8}(1+x)^{-2} - \frac{3}{4}(1+x)^{-4} + \frac{15}{128}(1+x)^{-6} \quad (12)$$

The interaction potential $V(x)$ as it usually written in DLVO theory is the sum of an attractive London–van der Waals interaction $V_A(x)$ and a repulsive interaction due to the electric charge of the spheres. The expression for $V_A(x)$ derived by Hamaker for the case of two spheres is

$$V_A = -\frac{A}{12} \left[(x^2 + 2x)^{-1} + (x^2 + 2x + 1)^{-1} + \frac{2 \ln(x^2 + 2x)}{(x^2 + 2x + 1)} \right] \quad (13)$$

where A is the attractive Hamaker constant. Two approximate expressions have been proposed for the repulsive interaction, $V_R(x)$, for the limiting cases of $\kappa a < 1$ and $\kappa a > 1$. We have used the expression

$$V_R(x) = \frac{\epsilon a \Psi_0^2}{2} \ln[1 + \exp(-2\kappa ax)] \quad (14)$$

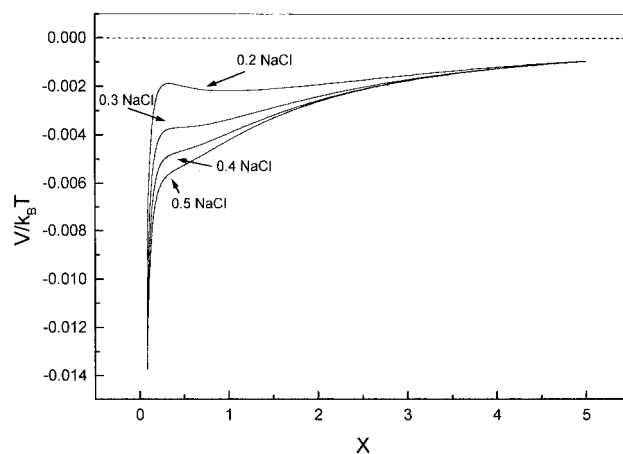
which is appropriate for values up to $\kappa a > 1$.

The aggregate charge, q , is related to the surface potential, Ψ_0 , by the expression²¹

$$\Psi_0 = (2k_B T/e) \sinh^{-1}[2\pi\epsilon\kappa^{-1}qe/4\pi a^2\epsilon k_B T] \quad (15)$$

Table 3. Experimental and Theoretical Slopes, k_D , and Reduced Potential, $e\Psi_0/k_B T$ as a Function of Electrolyte Concentrations Calculated Considering (a) Only Counterions from Electrolyte and (b) Counterions from Both Electrolyte and Surfactant (in parenthesis)

[NaCl] (mol kg ⁻¹)	k_D		$e\Psi_0/k_B T$
	experimental	theoretical	
0.0	-0.41	— (-0.32)	— (0.83)
0.2	-0.54	-0.48 (-0.65)	0.30 (0.68)
0.3	-0.62	-0.77 (-0.69)	0.22 (0.64)
0.4	-0.82	-0.87 (-0.83)	0.15 (0.52)
0.5	-1.07	-0.91 (-0.97)	0.09 (0.39)

**Figure 6.** Plots of the pair interaction potential $V(x)$ as a function of the reduced and normalized distance x at different electrolyte concentrations, taking into account only counterions from electrolyte.

The computational procedure involved iterations of values of A and Ψ_0 to give the best fit of computed and experimental values of k_D over the range of electrolyte concentration.

For our initial calculations we considered only those counterions from the electrolyte, as is usual for such computations. The value of q derived from eq 14 was 0.01 units of electron charge (uec) and the Hamaker constant was 0.18×10^{-21} J. Agreement between computed and experimental k_D values was reasonable in view of the assumptions inherent in these calculations (Table 3). In Figure 6 we show the behavior of $V(x)/k_B T$ for a set of electrolyte concentrations. This potential is always negative and seems to indicate a precipitation of the system, which is in contradiction with the low aggregation number obtained from light scattering and the experimental observation. However, when the counterions from SHS were included as well as those from the electrolyte, the values of q and A were 0.10 uec and 0.21×10^{-21} J, respectively, and the predicted effect of electrolyte on the reduced potential, $e\Psi_0/k_B T$, and $V(x)/k_B T$ were closer to experimental results, as seen from Table 3 and Figure 7. These calculations show the importance of including the surfactant counterions in the prediction of interactive forces when, as is the case here, the cc is high and the contribution of counterions from added electrolyte and from surfactant is of similar order. Figure 7 shows the predominance of electrostatic repulsion at low electrolyte concentration. At increasing electrolyte concentration the electrostatic potential is screened and London–van der Waals attraction becomes increasingly important.

The values calculated for the Hamaker constants of the aggregates of sodium *n*-hexyl sulfate are comparable to those of other systems of low aggregation number, for

(20) Felderhof, B. U. *J. Phys.* **1978**, *11*, 929.(21) Szajdzinska-Pietek, E.; Maldonado, R.; Kevan, L.; Jones, R. R. M. *J. Colloid Interface Sci.* **1986**, *110*, 514.

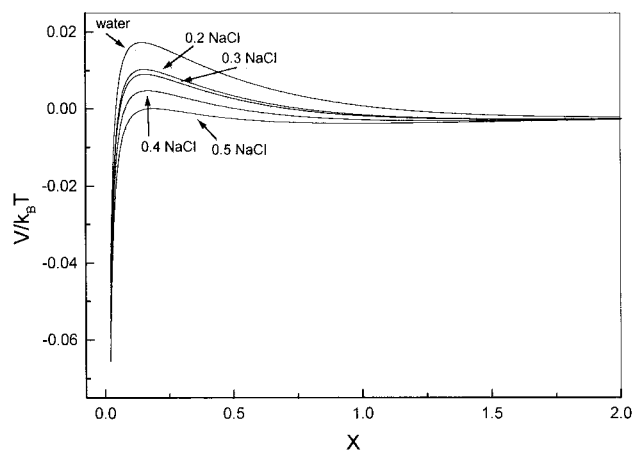
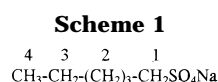


Figure 7. Plots of the pair interaction potential $V(x)$ as a function of the reduced and normalized distance x at different electrolyte concentrations, taking into account counterions from electrolyte and sodium *n*-hexyl sulfate.



example, the drugs chlorpromazine hydrochloride²² (1.30×10^{-21} J), promethazine hydrochloride²² (4.50×10^{-21} J), thioridazine hydrochloride²² (1.80×10^{-21} J), and propranolol hydrochloride²³ (0.20×10^{-21} J). These values are all appreciably lower than that of sodium dodecyl sulfate⁴ (45×10^{-21} J). A similar tendency was found for reduced potential values when compared with SDS⁴ (2.93 to 1.38 in the range of 0.1 to 0.5 mol kg⁻¹ NaCl), chlorpromazine hydrochloride²² (2.45 to 0.56 in the range of 0.00 to 0.1 mol kg⁻¹ NaCl), and thioxidazine hydrochloride²² (1.78 to 1.20 in the range of 0.025 to 0.050 mol kg⁻¹ NaCl), reflecting the large differences in the size of the aggregated species.

The self-association characteristics of sodium *n*-hexyl sulfate were further investigated using high-resolution NMR spectroscopy. The assignment of spectral lines was done by comparison with literature spectra.^{24–27} The chemical shifts of four selected positions (see Scheme 1) were measured as a function of solution concentration from ¹H NMR spectra of SHS solutions at a range of concentrations well below and above the *cc*.

Plots of the chemical shift as a function of the inverse of the total surfactant concentration show pronounced upfield shifts upon aggregation for protons in positions 1, 2, and 3, but a corresponding downfield shift for the proton in position 4 (Figure 8). Below the *cc*, no concentration dependence of the chemical shift was found for any position; when the concentration exceeds the *cc* the chemical shifts changed linearly with the reciprocal of the total concentration. Critical concentrations were determined from the intersection of the linear portions of the plots at concentrations above and below the inflection

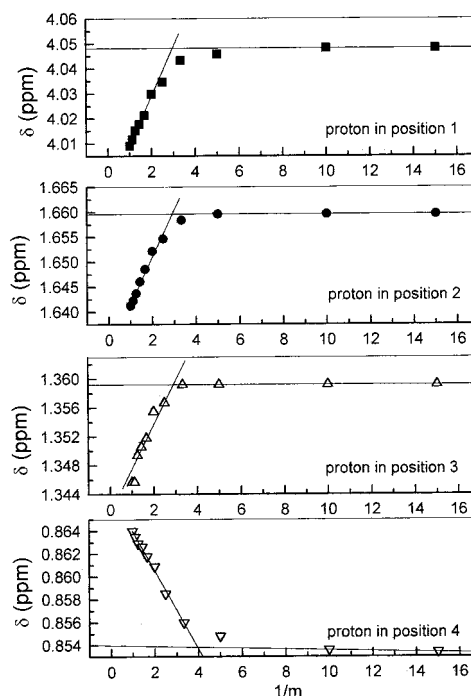


Figure 8. Variation of the ¹H chemical shift for the four positions along the sodium *n*-hexyl sulfate molecule as a function of the reciprocal concentration in NaCl solution with a concentration of 0.5 mol kg⁻¹.

Table 4. Critical Concentrations (*cc* in mol kg⁻¹) and Aggregation Numbers (*N*) from NMR Chemical Shifts the Four Selected Protons along the Alkyl Chain (see Scheme 1)

[NaCl] (mol kg ⁻¹)	proton in position 1		proton in position 2		proton in position 3		proton in position 4	
	<i>cc</i>	<i>N</i>	<i>cc</i>	<i>N</i>	<i>cc</i>	<i>N</i>	<i>cc</i>	<i>N</i>
0.00	0.52	1	0.52	2	0.69	1	0.40	2
0.2	0.47	2	0.51	2	0.68	1	0.38	3
0.3	0.43	4	0.45	6	0.57	3	0.35	4
0.4	0.36	6	0.38	7	0.41	6	0.27	6
0.5	0.34	11	0.34	8	0.35	9	0.26	8

region and are listed in Table 4. Comparison with *cc* from static light scattering (Table 1) shows the closest agreement for values determined from the proton in the middle of the alkyl chain (position 3).

Values obtained for the *cc* in water at 25 °C by static light scattering and NMR are of similar order to those obtained in our previous study³ from conductivity measurements (0.559 mol kg⁻¹), apparent and partial molar volumes (0.48 mol kg⁻¹), and ultrasound measurements (0.471 mol kg⁻¹), compared with a literature value¹⁴ of 0.42 mol dm⁻³.

The magnitude of the chemical shift change, $\Delta\delta$ ($\Delta\delta = \delta_{\text{aggregate}} - \delta_{\text{monomer}}$), on aggregation at each electrolyte concentration, calculated for each position from the differences between the aggregate value, and that for the monomers are shown in Figure 9. It is interesting to note a lack of any significant dependency of $\Delta\delta$ on electrolyte concentration and hence on the size of the aggregate. From the inspection of Figures 7 and 8 we deduce that the greatest change of chemical shift is with the proton at the polar head rather than in the middle of the alkyl chain as reported for the micellization of sodium hexanoate, sodium octanoate, nonylammonium bromide, and potassium *N*-*n*-dodecanonyl-D-alaninate,^{28,29} suggesting differences in aggregate structure for sodium *n*-hexyl sulfate.

(28) Desando, M. A.; McGarvey, B.; Reeves, L. W. *J. Colloid Interface Sci.* **1996**, *181*, 331.

(22) Attwood, D.; Blundell, R.; Mosquera, V. *J. Colloid Interface Sci.* **1993**, *157*, 50.

(23) Ruso, J. M.; Attwood, D.; Rey, C.; Taboada, P.; Mosquera, V.; Sarmiento, F. *J. Phys. Chem.* **1999**, *103*, 7092.

(24) Williams, D. H.; Fleming, I. In *Spectroscopy Methods in Organic Chemistry*, 5th ed.; McGraw-Hill: New York, 1995.

(25) Bhacca, N. S.; Johnson, L. F.; Shoolley, J. N. *High Resolution NMR Spectra Catalogue*; Varian Associates: Palo Alto, CA, 1963; Vols. I and II.

(26) Pouchert, C. J. *The Aldrich Library of NMR Spectra*, 2nd ed.; Aldrich Chemical Co. Inc., 1983; Vols. 1 and 2.

(27) Pretsch, E.; Clerc, T.; Seibl, J.; Simon, W. *Tables of Spectral Data for Structure Determination of Organic Compounds*, English ed.; Springer: Berlin, 1983.

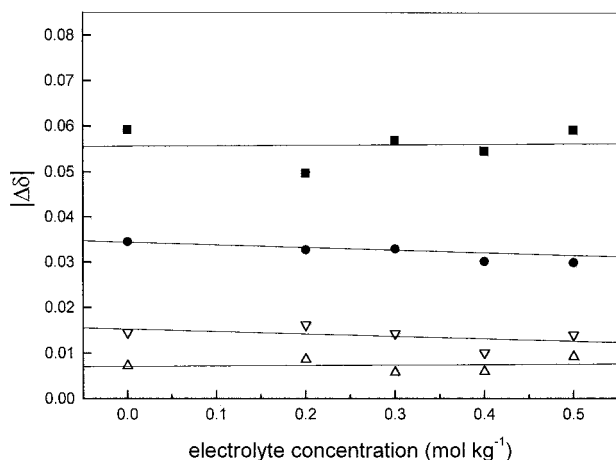


Figure 9. Plots of ^1H difference chemical shift between micellar and monomeric states against electrolyte concentration. (■) proton in position 1; (●) proton in position 2; (△) proton in position 3; and (▽) proton in position 4.

Based on the mass action law, the chemical shift can be written³⁰

$$\delta_{\text{obsd}} = \frac{m_m}{m} \delta_m \quad (16)$$

where m_m and m are the concentration of aggregated surfactant and the total surfactant concentration, respectively. δ_{obsd} is the observed chemical shift and δ_m the shift of aggregated surfactant, both taken relative to the chemical shift of the monomer, calculated as the extrapolation to zero surfactant concentration. It is possible to express the concentration of monomer as

$$[A] = m \frac{\delta_m - \delta_{\text{obsd}}}{\delta_m} \quad (17)$$

and the aggregate concentration as

(29) Persson, B.-O.; Drakenberg, T.; Lindman, B. *J. Phys. Chem.* **1979**, *83*, 3011.

(30) Persson, B.-O.; Drakenberg, T.; Lindman, B. *J. Phys. Chem.* **1976**, *80*, 2124.

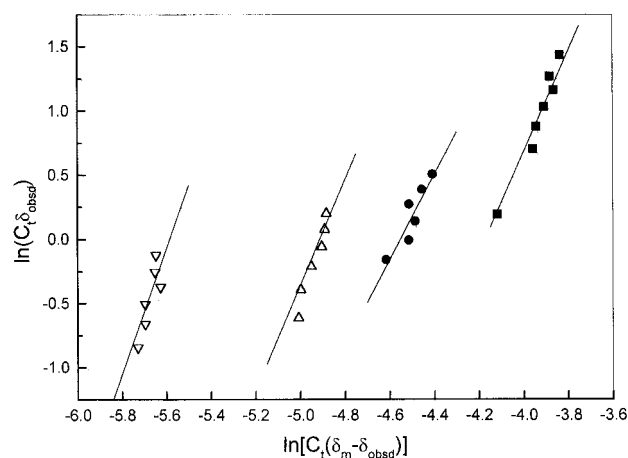


Figure 10. NMR chemical shift data plotted according to eq 18 for sodium *n*-hexyl sulfate in 0.5 mol kg⁻¹ NaCl solution. (■) proton in position 1; (●) proton in position 2; (△) proton in position 3; and (▽) proton in position 4.

$$N[A_N] = m \frac{\delta_{\text{obsd}}}{\delta_m} \quad (18)$$

Then the expression for K may be expressed as

$$\ln(m\delta_{\text{obsd}}) = N \ln[m(\delta_m - \delta_{\text{obsd}})] + \ln K + \ln N - (N - 1) \ln \delta_m \quad (19)$$

Plots of $\ln(m\delta_{\text{obsd}})$ against $\ln[m(\delta_m - \delta_{\text{obsd}})]$ can therefore, in principle, yield the aggregation number and the equilibrium constant. A representative plot is shown in Figure 10, and similar plots were obtained at each electrolyte concentration. The aggregation numbers calculated using chemical shifts for the four positions at each electrolyte concentration are shown in Table 4 and are in reasonable agreement with corresponding values from static light scattering.

Acknowledgment. The authors thank the Xunta de Galicia for financial support.

LA990721F